Hindawi
Journal of Chemistry
Volume 2020, Article ID 5238501, 21 pages
https://doi.org/10.1155/2020/5238501

Research Article

Synthesis, Characterization, Cyclic Voltammetry, and Biological Studies of Co(II), Ni(II), and Cu(II) Complexes of a Tridentate Schiff Base, 1-((E)-(2-Mercaptophenylimino) Methyl) Naphthalen-2-ol (H_2L_1)

Maurice Kuate,[1,2] **Mariam Asseng Conde**,[2] **Evans Ngandung Mainsah**,[3] **Awawou G. Paboudam**,[1] **Francis Merlin M. Tchieno**,[4,5] **Kevin I. Y. Ketchemen**,[1] **Ignas Tonle Kenfack**,[4] **and Peter T. Ndifon**[1]

[1]*Department of Inorganic Chemistry, Faculty of Science, University of Yaounde I, Yaounde, Cameroon*
[2]*Department of Chemistry, Faculty of Science, University of Douala, Douala, Cameroon*
[3]*Department of Chemistry, Faculty of Science, University of Buea, Buea, Cameroon*
[4]*Department of Chemistry, Faculty of Science, University of Dschang, Dschang, Cameroon*
[5]*Department of Chemistry, Faculty of Science, University of Maroua, Maroua, Cameroon*

Correspondence should be addressed to Peter T. Ndifon; pndifon@yahoo.com

Received 24 March 2020; Revised 20 July 2020; Accepted 24 October 2020; Published 9 November 2020

Academic Editor: Radhey Srivastava

Copyright © 2020 Maurice Kuate et al. This is an open access article distributed under the Creative Commons Attribution License, which permits unrestricted use, distribution, and reproduction in any medium, provided the original work is properly cited.

A novel tridentate Schiff base, 1-((E)-(2-mercaptophenylimino) methyl) naphthalen-2-ol (H_2L_1), was synthesized by the condensation reaction of 2-hydroxy-1-naphthaldehyde with 2-aminothiophenol in absolute ethanol. The resulting ligand was reacted with Co(II), Ni(II), and Cu(II) ions to obtain tetrahedral CoL_1, NiL_1, and square planar CuL_1 complexes. The Schiff base and its metal complexes were characterized using ^{1}H-NMR, microanalysis, FT-IR, UV-visible, and mass spectroscopy (ESI-MS). All the compounds are soluble in DMSO and DMF. Spectroscopic studies show that the ligand coordinates to the metal center through the azomethine nitrogen, naphthoxide oxygen, and thiophenoxide sulfur to form a tridentate chelate system. Conductance measurements show that these compounds are molecular in solution. Cyclic voltammetry studies show Co(III)/Co(II) and Cu(II)/Cu(I) redox systems to be quasi-reversible involving a monoelectronic transfer while Ni(III)/Ni(II) was irreversible. *In vitro* antibacterial and antifungal activity against five bacterial strains (*Escherichia coli, Staphylococcus aureus, Pseudomonas aeruginosa, Enterococcus faecalis,* and *Proteus mirabilis*) and five fungal strains (*Candida albicans*, *Candida glabrata, Candida tropicalis, Candida krusei*, and *Candida parapsilosis)* showed no antifungal activity but moderate antibacterial activity on *E. coli, S. aureus, P. aeruginosa,* and *P. mirabilis* bacterial strains. Antioxidant studies reveal that the ligand and its Cu(II) complex are more potent than Co(II) and Ni(II) complexes to eliminate free radicals.

1. Introduction

The synthesis, structure, and reactivity of Schiff bases have generated a lot of interest due to their ease of preparation and structural flexibility. Schiff bases are known to possess potential applications in biological modeling, catalysis, design of molecular magnets, and the synthesis of therapeutic agents [1–4]. Schiff bases have also been shown to exhibit a broad range of biological activities, including antifungal, antibacterial, antioxidant, and anti-inflammatory properties [4–9]. The common structural feature of Schiff's bases is the presence of the characteristic azomethine functionality, RHC = NR′, which has been shown to account for the observed pharmacological activities [4]. Schiff bases of salicylaldehyde derivative behave generally as bidentate ligands and coordinate through the oxygen atom of the phenolic

group and the nitrogen atom of the azomethine group. Schiff bases are found to be the most appropriate chelating ligands in coordination chemistry due to their ability to bond through N, O, and/or S atoms [5, 6] as either bidentate or tridentate chelators which typically form four- or six-coordinate complexes.

The stabilization of metal centers using bidentate mixed donor Schiff bases involving N- and *O*-donors has been extensively studied [5–8]. Most tridentate donor ligands have been shown to stabilize metal ion centers, forming strain-free five- or six-membered rings [9, 10].

The increasing resistance of microbes to antibacterial and antifungal drugs has necessitated the search for new compounds to target these pathogens. The incorporation of metal-based systems into organic molecules is expected to enhance the biological properties of these drugs. Complexes of Schiff bases have been extensively studied as potential antibacterial, antifungal, and anticancer agents [11–13]. Tridentate Schiff base complexes having oxygen, nitrogen, and sulfur donor atoms have been reported to possess unusual structure [14], antimicrobial [15, 16], anti-inflammatory [17, 18], antiviral, anticancer [19], and electrochemical properties [20, 21]. In recent years, tridentate Schiff bases derived from aminophenol received enormous attention as ligands due to their metal-binding ability and their various applications. Our group has recently embarked on studies on the biological activities of complexes of heterocyclic Schiff base ligands [15, 22]. One such class of heterocyclic Schiff base ligands is the pyridine carboxaldehyde isonicotinoyl hydrazones, derived from isoniazid (isonicotinic acid hydrazide) which are generally bidentate or tridentate chelators and typically form six-coordinate complexes [22–24].

In continuation of our studies on metal complexes of aromatic Schiff base ligands, we report, herein, the synthesis and electrochemical studies of Co(II), Ni(II), and Cu(II) complexes of a tridentate Schiff base derived from 2-aminothiophenol and 2-hydroxy-1-naphthaldehyde and the evaluation their antioxidant and antimicrobial properties.

2. Experimental

2.1. Materials and Measurements. All reagents and solvents were obtained from commercial sources and used without any further purification. Microanalysis (C, H, and N) data were obtained using a Perkin-Elmer model 240C elemental analyzer. Infrared spectra were determined using KBr pellets on an FTIR spectrophotometer Shimadzu model 8400s in the region 4000–400 cm^{-1}. Electronic spectra were recorded in DMSO on UV-Vis spectrophotometer spectroScan 80D in a 200–800 nm range. ^{1}H-NMR for the ligand was recorded on a Bruker AMX 300 spectrometer operating at 300.13 MHz using DMSO-d_6 as solvent and TMS as a standard reference. The high-resolution mass spectrum was obtained with a Waters Micromass LCT Premier Mass Spectrometer in Electron Spin ionization (ESI) mode. The cyclic voltammograms were recorded on a μ-Autolab III potentiostat using a conventional three-electrode cell. A glassy carbon electrode was used as the working electrode while Ag/AgCl and platinum gauze were employed as the reference and auxiliary electrodes, respectively. A 0.1 M H_2SO_4 solution was used as the supporting electrolyte, and all synthesized compounds were dissolved in DMF. All electrochemical measurements were carried out in solutions containing 10^{-3} M for either the ligand or its metal complexes. These solutions were degassed with N_2 prior to any recording of cyclic voltammograms while maintaining them under an inert atmosphere.

2.2. Synthesis. The Schiff base ligand and its complexes were synthesized according to the general synthetic procedure [25, 26].

2.2.1. Synthesis of Schiff Base (H_2L_1). The Schiff base (H_2L_1) was synthesized by the condensation of 2-aminothiophenol and 2-hydroxy-1-naphthaldehyde. An ethanolic solution of 2-hydroxy-1-naphthaldehyde (3,271 g; 19 mmol) was slowly added to an ethanolic solution of 2-aminothiophenol (2 mL; 19 mmol). The reaction mixture was maintained under reflux for two hours. The volume of the resulting yellow solution was reduced by evaporation and cooled in ice water. The yellow precipitate formed was filtered, washed several times with ethanol, and air-dried. The yellow product was collected: Yield: 92%; m.p 160°C; Analysis for $C_{17}H_{13}NOS$ (%); Found (calc): C, 73.00 (73.09); H, 4.43 (4.69); N, 4.90 (5.01); ESI-MS in methanol: *m/z* 279.2.

2.2.2. Synthesis of the Complexes. All complexes were synthesized using the same procedure. 1.00 mmol of metal nitrate hydrate was dissolved in 10 mL ethanol and added dropwise to a vigorously stirring (1.00 mmol) methanolic solution of ligand H_2L_1. The resulting solution was stirred under reflux for two hours and cooled. The colored precipitate of each complex was obtained, filtered, washed thoroughly with ethanol, and air-dried at room temperature.

2.3. Electrochemical Studies. Cyclic voltammetry studies were carried out on a μ-Autolab (type III) potentiostat, with a three-electrode cell containing a glassy carbon as the working electrode, an Ag/AgCl reference electrode, and Pt foil counter electrode. Prior to each experiment, the glassy carbon electrode was properly cleaned by polishing using an Al_2O_3 suspension. Solutions of the Schiff base ligand and complexes (1.0×10^{-3} M) in DMF with sulfuric acid (0.1 M) as a supporting electrolyte were degassed using dry nitrogen gas for 15 minutes and then blanketed with the same gas during the experiments. All compounds were investigated at room temperature. The voltammograms were recorded at a potential scan rate of 100 $mV \cdot s^{-1}$.

2.4. In Vitro Antioxidant Activity. The ligand, H_2L_1, and its complexes were tested for *in vitro* antioxidant activities at 37°C using DPPH free radical scavenging assay [27] with some modifications. Solutions of the ligand and complexes at different concentrations (200, 100, 50, 25.5, and 12.25 μg/

mL) were prepared in methanol as solvent. 1 mL of each sample at different concentrations and 540 μL of DPPH (0.08 mg/mL) solution were measured into different test tubes, and the mixture was shaken vigorously for about 2-3 minutes. The contents of the test tubes were then incubated in the dark for 30 minutes at room temperature. A blank DPPH solution without the sample used for the baseline correction gave a strong absorption maximum at 517 nm (purple color with $\varepsilon = 8.32 \times 10^3\,\mathrm{M}^{-1}\cdot\mathrm{cm}^{-1}$). After incubation, the absorbance value for each sample 510–520 nm was measured using a UV-visible spectrometer. The observed decrease in absorbance values indicates that the compounds show scavenging activity and the relative free radical scavenging effects were calculated using the formula [28]:

$$\text{scavenging effects}\,(\%) = \frac{\left[\mathrm{Abs}_{\mathrm{control}} - \mathrm{Abs}_{\mathrm{sample}}\right]}{\mathrm{Abs}_{\mathrm{control}}} \times 100, \tag{1}$$

where $\mathrm{Abs}_{(\mathrm{control})}$ is the absorbance of DPPH radical + DMF and $\mathrm{Abs}_{(\mathrm{sample})}$ is the absorbance of DPPH radical + sample (test samples/standard). Each analysis was made in triplicate, and the obtained mean data were compared with Trolox values used as standard.

2.5. Antimicrobial Study. The Schiff base ligand and its respective metal(II) complexes were screened for *in vitro* antibacterial and antifungal activity against some bacterial strains (*Escherichia coli, Staphylococcus aureus, Pseudomonas aeruginosa, Enterococcus faecalis,* and *Proteus mirabilis)* and some fungal strains (*Candida albicans*, *Candida glabrata, Candida tropicalis, Candida krusei*, and *Candida parapsilosis)*; Ciprofloxacin and Ketoconazole (at 1 mg/ml in DMSO) were used as antibacterial and antifungal references, respectively.

2.5.1. Determination of the Diameters of Zone of Inhibition. The diameters of the zone of inhibition of the synthesized ligand and its complexes were determined using the agar well diffusion method [29, 30]. The stock solutions (1 mg/mL) of the compounds were prepared in DMSO. For the determination of the zone of inhibition, the medium was poured into the Petri dish and allowed to solidify at room temperature. Wells were made on the solidified medium, and the prepared solutions were added to the wells and allowed to diffuse into the wells. The indicator organisms were overlaid on to the agar medium, and the plates were incubated at 37°C for 24 hours for the bacteria and 48 hours for the yeasts. The antimicrobial activities were assessed by measuring the diameter of the zone of inhibition of the bacterial and fungal growth around every well with a ruler following two axes. For every product tested, three determinations were done.

2.5.2. Minimum Inhibitory Concentration. The minimum inhibitory concentrations (MICs) were determined by the method of microdilution in a liquid environment in the 96-well microtiter plates for the bacterial species [31]. The quantitative antifungal activities of the test compounds were evaluated using the microdilution broth method [32]. Twofold serial dilutions of the compounds were prepared in 96-well microtiter plates using sterile nutrient broth as diluent. The plates were inoculated with 100 μL bacterial or fungal suspensions containing 1.5×10^8 colony-forming units (CFUs) [32] and incubated at 37°C for 48 hours for fungal species and 24 hours for bacterial species. The MIC value was defined as the lowest concentration of the compounds giving complete inhibition of visible growth.

3. Results and Discussion

The ligand H_2L_1 was prepared by condensing equimolar amounts of 2-aminothiophenol with 2-hydroxy-1-naphthaldehyde in absolute ethanol under reflux (see Scheme 1).

The corresponding Co(II), Ni(II), and Cu(II) complexes were synthesized in 1 : 1 molar ratio of the Schiff base ligand and the metal(II) ions using $M(NO_3)_2 \times H_2O$. The ligand is soluble in methanol and hot ethanol while both the ligand and its complexes are soluble in DMF and DMSO. The analysis and physical properties of the prepared compounds are given in Table 1.

The yellow color of the ligand has been used to predict the formation of the Schiff base. Elemental analysis values for the ligand and its complexes (Table 1) tallied with the expected values, thus confirming the purity of the compounds and the formation of the Schiff base ligand. A 1 : 1 reaction ratio for metal ion and the ligand during the formation of the complexes was proposed. Thus, the complexes were of the form [ML], which may thus dimerize [33, 34], to form a neutral dimeric four-coordinate complex $[ML]_2$. The dimerization is presumed to occur as a result of bridging between the two M(II) centers through the deprotonated thiophenolic sulfur atoms. The very low molar conductivities of the synthesized compounds in DMSO indicated that all complexes are molecular in nature.

3.1. Infrared Study. The infrared spectrum of the ligand is presented in Figure 1 and the data are summarized in Table 2. The infrared spectrum of the ligand exhibits absorption bands around 3255 and 2943 cm^{-1} which are attributed to the hydroxyl and thiol groups, respectively. The broad nature of the bands indicates the existence of an intramolecular hydrogen bonding between the O-H and nitrogen atom of -C=N groups [34]. The loss of absorption band at 3317–3385 cm^{-1} for $\nu_{(\mathrm{N\text{-}H})}$ stretch of 2-aminothiophenol and at 1706 cm^{-1} for $\nu_{(\mathrm{C=O})}$ of 2-hydroxy-1-naphthaldehyde and appearance of a peak at 1612 cm^{-1} attributed to azomethine group $\nu_{(\mathrm{C=N})}$ in the ligand are indicative of the formation of the Schiff base, H_2L_1.

The IR spectrum of the ligand has been compared with the IR spectra of metal complexes (Figure S1) that revealed the binding modes of the ligand to metal ions, which is confirmed by the change in the positions of absorption bands. The strong band at 1612 cm^{-1} attributed to the imine $\nu_{(\mathrm{C=N})}$ functional group of the free ligands was redshifted, to

Table 1: Analysis and physical properties of Schiff base and the corresponding complexes.

Compounds	Color	Yield (%)	Melting point (°C)	Molar mass ($g \cdot mol^{-1}$)	% found (calculated)			Λ_m ($\Omega^{-1} \cdot cm^2 \cdot mol^{-1}$)
					C	*H*	*N*	
H_2L_1	Yellow	92.00	160	279.36	73.00 (73.09)	4.43 (4.69)	4.90 (5.01)	0.6
CuL_1	Dark green	61.70	>360	681.77	61.34 (59.90)	3.03 (3.25)	4.07 (4.11)	2.0
CoL_1	Dark brown	65.50	>360	686.06	59.47 (59.52)	3.42 (3.45)	3.96 (4.08)	1.2
NiL_1	Red	64.40	>360	672.07	60.64 (60.76)	3.28 (3.30)	3.98 (4.17)	0.8

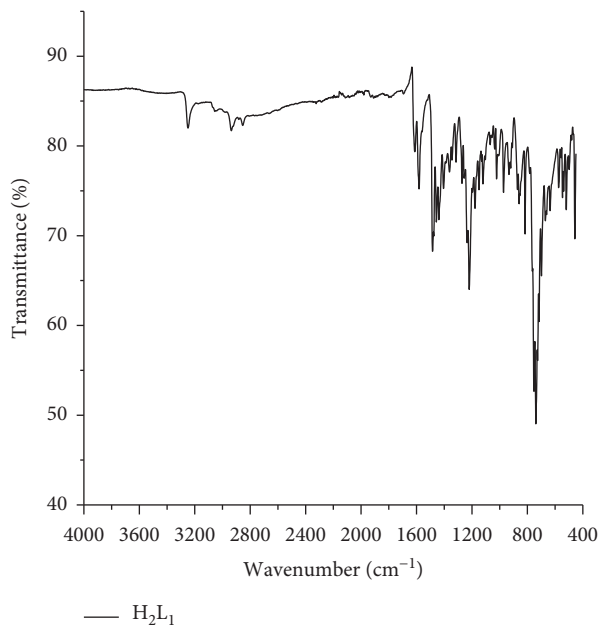

Figure 1: Infrared spectrum of the ligand H_2L_1.

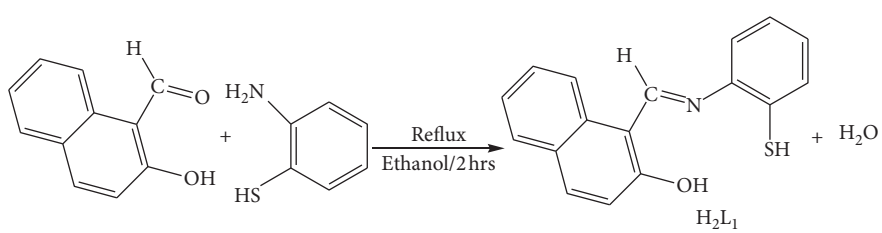

Scheme 1: Reaction equation of synthesis of the Schiff base.

Table 2: Infrared data of the Schiff base (H_2L) and its corresponding complexes.

Compounds	$\nu_{C=N}$	ν_{C-O}	ν_{C-S}	$\nu_{C-S\ asym}$	ν_{O-H}	ν_{S-H}	ν_{M-N}	ν_{M-O}	ν_{M-S}	ν_{H2O}
H_2L_1	1612	1238	738	817	3255	2943	—	—	—	—
CuL_1	1600	1348	741	824	—	—	522	561	456	—
CoL_1	1600	1360	747	837	—	—	501	555	468	3452
NiL_1	1608	1375	746	821	—	—	508	575	454	—

1608–1600 cm^{-1}, in the complexes and indicative of the involvement of the imine nitrogen atom in coordination [34, 35]. The disappearance of the absorption bands around 3255 and 2943 cm^{-1} attributed to O-H and S-H groups in the spectra of the complexes is due to deprotonation and involvement of the oxygen and sulfur atoms in the coordination to metal ion [34, 35], thus confirming the tridentate nature of the ligand. This is further supported by the appearance of three new bands at 522–501 cm^{-1}, 575–555 cm^{-1}, and 468–454 cm^{-1} in the far-infrared spectra of the complexes, assigned to $\nu_{(M\text{-}N)}$, $\nu_{(M\text{-}O)}$ and $\nu_{(M\text{-}S)}$, respectively [34–36]. In addition, the broad absorption peak observed at 3452 cm^{-1} in the Co(II) complex is attributed to O-H of the water molecule of crystallization.

3.2. ^{1}H NMR Spectral Analysis. ^{1}H-NMR spectra of the ligand and metal complexes confirmed the binding of the Schiff base with metal ions (Ni(II), Co(II), and Cu(II)). The intensities of each signal in the ^{1}H-NMR spectra of the ligand and its metal complexes were proportional as expected to the number of different types of protons present. The ^{1}H-NMR data of the compounds and the chemical shifts of the different types of protons are listed in Table 3.

The ^{1}H-NMR spectrum of the ligand is presented in Figure 2. The phenolic proton of the ligand appears downfield as a singlet at 15.01 ppm while the signal at 3.35 ppm was attributed to the thiol (-SH) proton. The broadness of the signal was due to a strong hydrogen bonding between the imine nitrogen and the phenolic proton [34–36]. On the other hand, the azomethine proton (-HC=N-) appeared as a strong singlet at 9.78 ppm, confirming the formation of the Schiff base. All the aromatic protons were observed at 7.89–7.02 ppm [38].

A comparison of ^{1}H-NMR spectra of copper, cobalt, and nickel complexes with that of the free ligand displayed an upfield shift in the signal of azomethine proton which appeared at 8.09–8.36 ppm suggesting the coordination of azomethine nitrogen to the metal ions [37]. However, signals at 15.01 ppm and 3.35 ppm corresponding to a hydroxyl group and thiol group, respectively, in free ligand were found to be absent in both complexes, indicating the deprotonation of the hydroxyl group of naphthaldehyde moiety and thiol group of 2-aminothiophenol [38]. However, the peak in the range 10-11 ppm corresponds to the possible enamine tautomerization proton. Moreover, the signal observed at 3.34 ppm, corresponding to two protons in Co(II) complex spectrum, is assigned to one water molecule of crystallization [38]. The above conclusion is in agreement with the IR analysis which confirmed that the ligand is tridentate and coordinates to the metal using the azomethine nitrogen, phenolic oxygen, and thiophenolic sulfur atoms. The ^{1}H-NMR data of the ligand and its complexes are presented in Table 3.

3.3. Mass Spectra. The ESI-MS of the Schiff base was performed to determine the molecular weight and fragmentation pattern. The molecular ion peak was observed at *m/z* 279.2 confirming formula weight ($C_{17}H_{13}NOS$) of H_2L_1. The peak at *m/z* 302.2 can be assigned to $[M + Na]^+$ and the peak at $m/z = 304.1$ is assigned to $[MH + Na]^+$ probable (^{13}C-isotope in this case, due to its very low relative abundance) [39]. The mass spectrum of H_2L_1 is shown in Figure 3.

3.4. Electronic Spectra. The UV-visible spectra of compounds are presented in Figure 4, and their electronic data in DMSO are given in Table 4. The spectrum of H_2L_1 exhibited high-intensity bands at 362 nm (27624 cm^{-1}), assigned to $\pi \longrightarrow \pi^*$ transition, and at 465 nm (21505 cm^{-1}) assigned to $n \longrightarrow \pi^*$ transition [39, 40]. The band at 362 nm in the spectrum of the Schiff base experienced a blue shift in the spectra of the complexes. The spectrum of CuL_1 complex shows an absorption band at 586 nm attributed to $^2B_{1g} \longrightarrow {}^2A_{1g}$ transition of square planar geometry around Cu(II) while the band observed at 436 nm was attributed to charge transfer transition [40]. The spectrum of CoL_1 complex shows an absorption band at 640 nm attributed to $^4A_2 \longrightarrow {}^4T_1(P)$ transition which corresponds to tetrahedral geometry, while the band observed at 476 nm corresponds to charge transfer transition [41–44]. The spectrum of NiL_1 showed absorption bands at 564 nm, attributed to $^3T_2(F) \longrightarrow {}^3T_1(F)$ transition which corresponds to tetrahedral geometry, and the band observed at 453 nm is charge transfer transitions [39].

3.5. Thermal Analysis. The differential and thermogravimetric analyses of CuL_1, CoL_1, and NiL_1 complexes were determined under a nitrogen gas inert atmosphere in the range 0 and 600°C. The thermograms and data obtained are shown in Figure 5 and Table 5, respectively. The thermal decomposition curves of CuL_1 and NiL_1 complexes showed single step decomposition corresponding to the loss of two molecules of ligand at 385°C (found: 72.11; calc: 72.56) and 428°C (found: 68.36; calc: 68.55), respectively, with a DTA of 400°C and 430°C, respectively. The thermal decomposition curve of the CoL_1 complex showed two-step decomposition. The first step at 220°C gave a loss (found: 15.12; calc: 15.11) which corresponds to one molecule of aminothiophenol, while the second step occurred in the range of 400–556°C (found: 44.05; calc: 44.10) corresponding to the loss of one molecule of aminothiophenol and two molecules of 2-hydroxy-1-naphthaldehyde [39].

3.6. Proposed Structures of Complexes. In agreement with microanalysis and all the spectroscopic results, the tridentate Schiff base coordinated to the metal using nitrogen atom of the azomethine group (-HC=N-), oxygen atom of hydroxynaphthaldehyde, and sulfur atom of the aminothiophenol. During the coordination, complexes probably dimerized to form neutral dimeric four-coordinate systems [33]. The dimerization is presumed to occur as a result of the bridging between the M(II) centers through the deprotonated thiophenolic sulfur atoms as described in Figure 6.

Table 3: ^{1}H-NMR data of ligand and its complexes.

Compounds	$\delta_{(O\text{-}H)}$	$\delta_{(N=C\text{-}H)}$	$\delta_{(S\text{-}H)}$	$\delta_{(Ar\text{-}H)}$	$\delta_{(H2O)}$
H_2L_1	15.01 ppm (s, 1H)	9.78 ppm (s, 1H)	3.35 ppm (s, 1H)	7.89–7.02 (m, 10H)	—
CuL_1	—	8.09 ppm (s, 1H)	—	7.25–6.45 (m, 10H)	—
CoL_1	—	8.36 ppm (s, 1H)	—	7.59–6.69 (m, 10H)	3.34 ppm (s, 2H)
NiL_1	—	8.31 ppm (s, 1H)	—	7.78–6.69 (m, 10H)	—

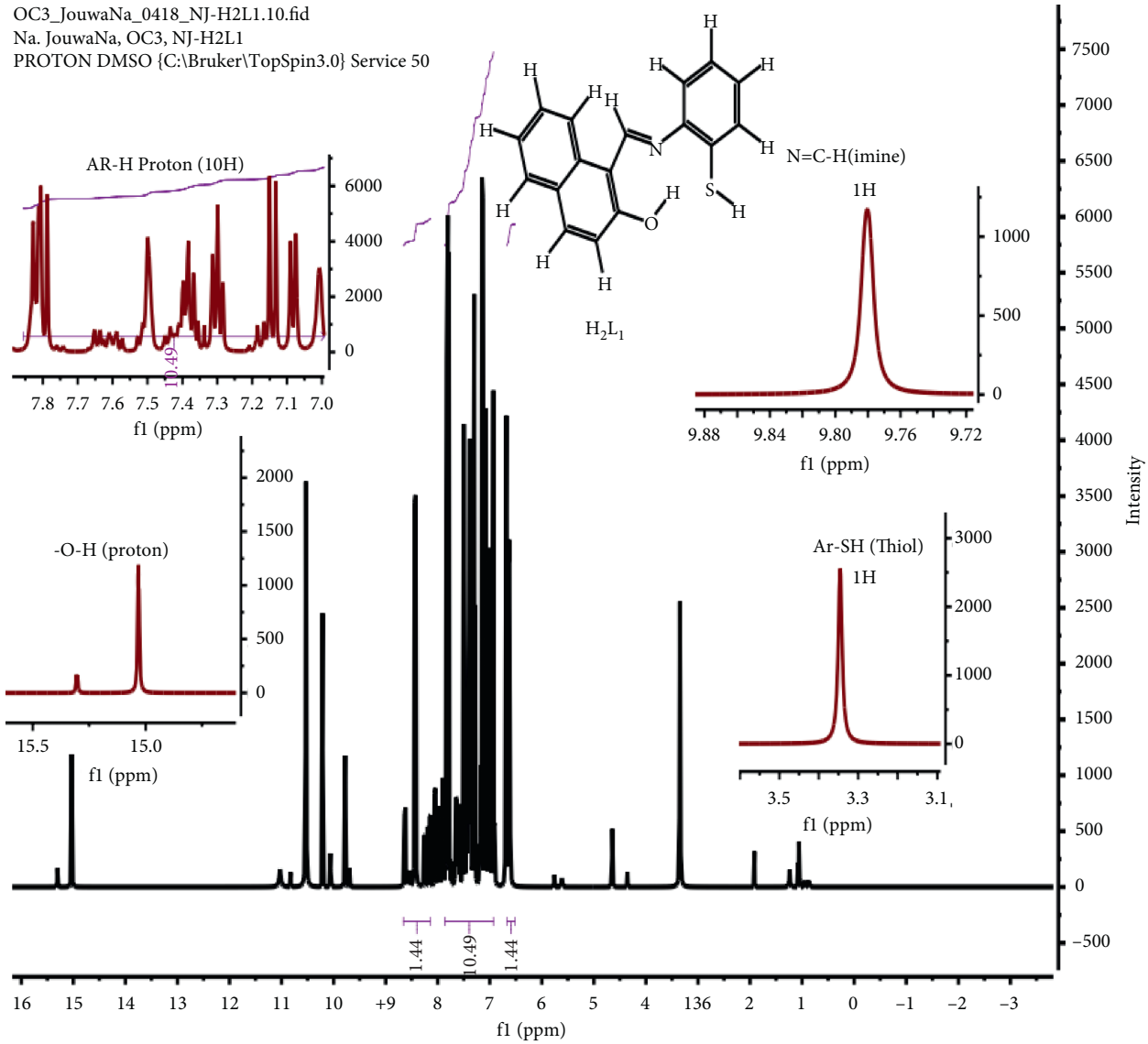

Figure 2: ^{1}H-NMR spectrum of the Schiff base ligand H_2L_1.

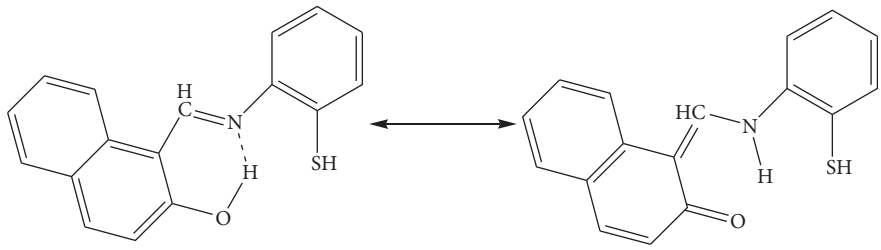

Scheme 2: Scheme showing the possibility of the Schiff base to tautomerize [31].

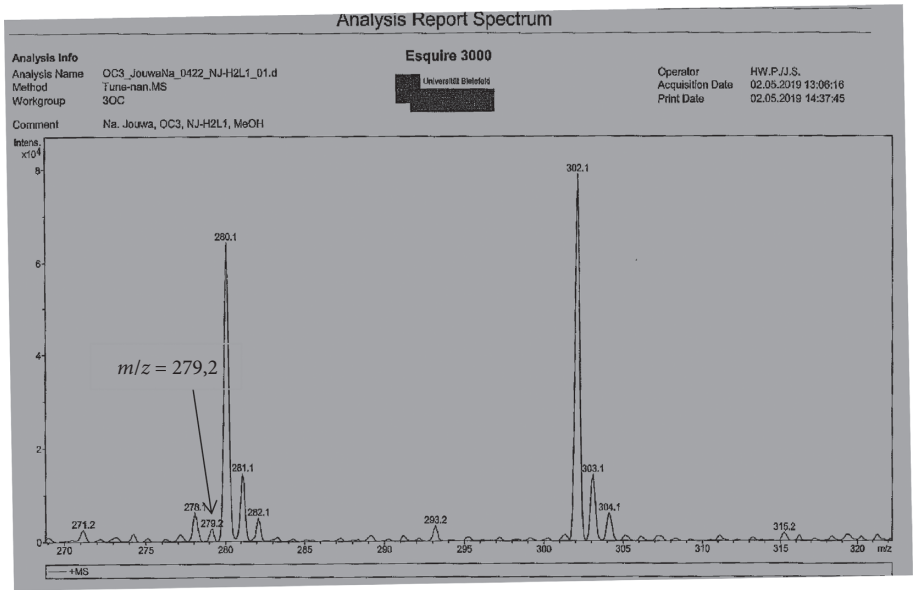

Figure 3: Mass spectra of the Schiff base ligand H_2L_1.

$$[Cu^{2+}(C_{17}H_{13}NOS)] + e^- \rightleftharpoons [Cu^{+}(C_{17}H_{13}NOS)]$$

Scheme 3: Electron transfer process in Cu(II) complex.

4. Cyclic Voltammetry Study

The electrochemical behavior of H_2L_1 and its Co(II), Ni(II), and Cu(II) complexes were investigated in DMF between −1.5 V and 1.5 V and a scan rate of 100 mV·s^{-1}.

4.1. Cyclic Voltammetry Study of Ligand H_2L_1. The cyclic voltammograms of the ligand (Figure 7) show three anodic waves at $E_{pa1} = 0.587$ V, $E_{pa2} = 0.897$ V, and $E_{pa3} = 1.105$ V. The first one, observed at 0.587 V, may be ascribed to the oxidation of the naphtone generated from the tautomeric equilibrium (Ketamine-Enamine) (see Scheme 2).

The last two waves at 0.897 and 1.105 V are attributed to the oxidation of thiophenolic and naphtholic groups, respectively [41–46]. For the return sweep, three cathodic waves were observed at 0.748, −0.141, and −1.075 V. The first wave observed at $E_{pc1} = 0.748$ V corresponds to the reduced species of the oxidized thiophenolic with naphtholic groups. The second wave is attributed to the naphtholic reduced form at $E_{pc2} = -0.141$ V while the third one observed at $E_{pc3} = -1.075$ V is attributed to the reduction of the azomethine group [41–46].

4.2. Cyclic Voltammetry Study of Cu(II) Complex. The cyclic voltammogram of CuL_1 complex (Figure 8) exhibits four oxidation peaks. The first peak at $E_{pa1} = 0.082$ V corresponds to the oxidation of Cu(I) to Cu(II), and the last three peaks at $E_{pa2} = 0.352$ V, $E_{pa3} = 0.943$ V, and $E_{pa4} = 1.174$ V are attributed to the oxidation of azomethine group, thiophenolic group, and naphtholic group, respectively [44]. On the cathodic side, two peaks were observed at $E_{pc1} = -0.346$ V and $E_{pc2} = -0.705$ V which correspond to the reduction of Cu(II) to Cu(I) and the reduction of the azomethine group, respectively [46]. When this cyclic voltammogram is compared to that of the ligand, the shift in the reduction potential of the azomethine group is observed. This confirms the involvement of the azomethine group in coordination. However, the oxidation potential of the thiophenolic and naphtholic moieties seems to be more positive than the value observed for the ligand, which may be related to the relative stability of the coordination bonding between the oxygen and sulfur atom with copper (II) ion [45]. The controlled potential electrolysis carried out shows that the peak corresponds to a one-electron transfer process, as given in Scheme 3.

4.3. Cyclic Voltammetry Study of Co(II) Complex. The cyclic voltammograms of CoL_1 complex (Figure 9) exhibit one oxidation peak at $E_{pa} = -0.603$ V corresponding to the oxidation of Co(II) to Co(III) and a reduction peak at $E_{pc} = -0.474$ V corresponding to the reduction of Co(III) to Co(II) [44–46]. When this cyclic voltammogram is compared to that of the ligand, a disappearance of the azomethine group reduction peak in the complex is observed. However, the oxidation potential of the thiophenolic and naphtholic moieties seems to be more positive than the value observed for the ligand which may be related to the relative stability of the coordination bonding between the oxygen and sulfur atom with cobalt (II) ion [46]. The controlled potential electrolysis carried out shows that the peak corresponds to a one-electron transfer process, as given in Scheme 4.

4.4. Cyclic Voltammetry Study of Ni(II) Complex. The cyclic voltammogram of NiL_1 complex (Figure 10) exhibits one oxidation peak at $E_{pa} = 0.840$ V corresponding to the

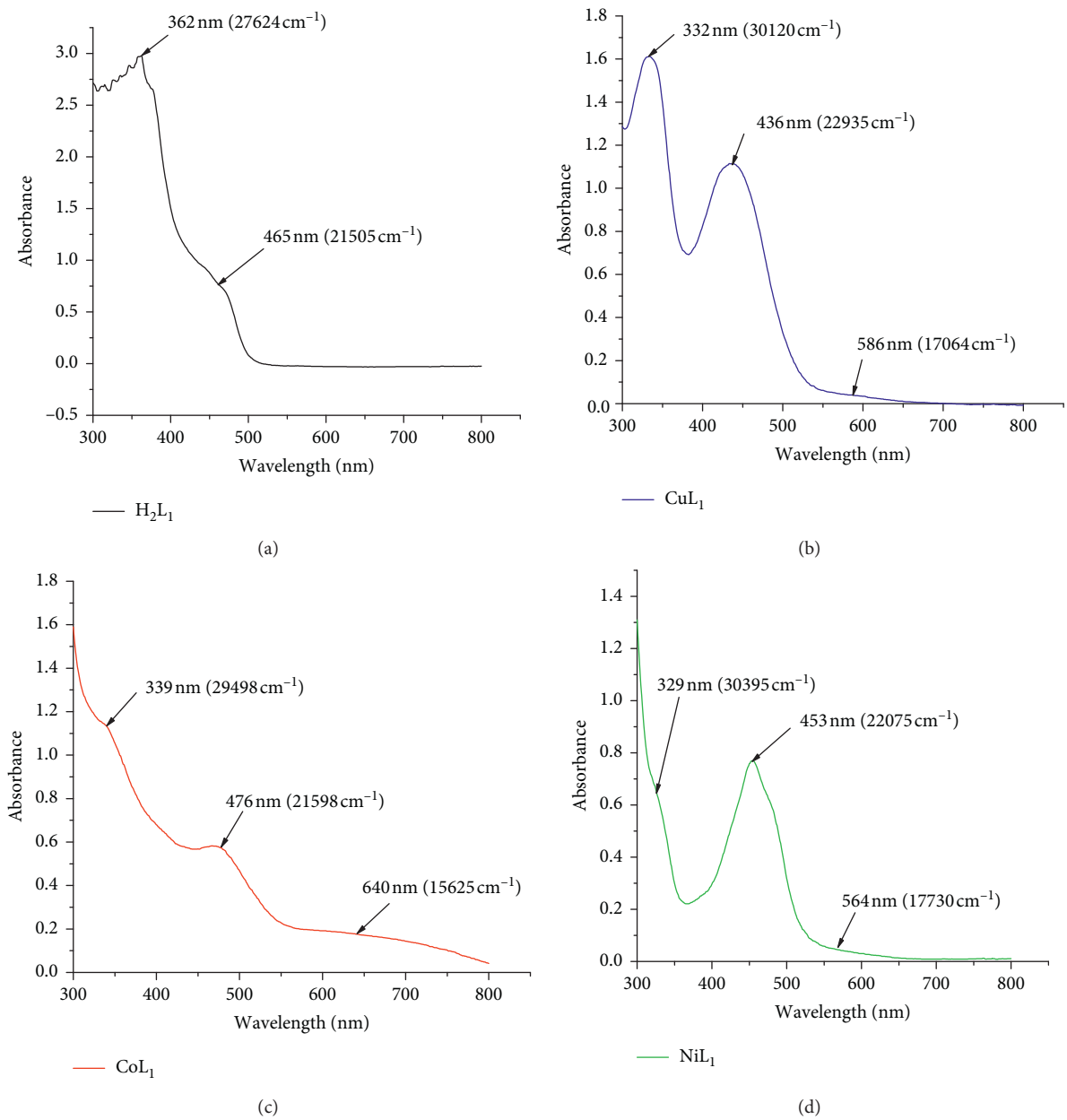

Figure 4: Electronic spectrum of ligand H_2L_1 and its corresponding complexes.

$$[Co^{3+}(C_{17}H_{13}NOS)] + e^- \rightleftharpoons [Co^{2+}(C_{17}H_{13}NOS)]$$

Scheme 4: Electron transfer process in Co(II) complex.

oxidation of Ni(II) to Ni(III) and a reduction peak observed at $E_{pc} = 0.487$ V corresponding to the reduction of Ni(III) to Ni(II) [46]. When this cyclic voltammogram is compared to that of the ligand, a disappearance of the azomethine group reduction peak in the complex is observed. However, the oxidation potential of the thiophenolic and naphtholic groups seems to be more positive than the value observed for the ligand [45]. The controlled potential electrolysis carried out shows that the peak corresponds to a one-electron transfer process, as given in Scheme 5.

In order to study the kinetics of the electrochemical process, the redox systems of the complexes were investigated separately in the reduced potentials range of −1 to 1.5 V using various scan rates (10 to 220 mV·s^{-1}). The obtained voltammograms are given in Figure 11. The peak-to-peak separation ΔEp of 0.428 V and 0.592 V for Cu(II)/Cu(I) and Co(III)/Co(II), respectively, indicates the quasi-reversibility of the redox system studied. The ratio of cathodic to anodic peak height was close to 1. However, the peak current increases with an increase in the square root of the scan rates (Figure 12). This establishes the electrode process as diffusion controlled. The ratio of cathodic to anodic peak height of redox couple Ni(III)/Ni(II) is greater than 1, which

Table 4: Electronic spectral data of the ligand and its corresponding complexes.

Compounds	λ (nm) and ν (cm^{-1})	ε ($L \cdot mol^{-1} \cdot cm^{-1}$)	Assignments	Suggested structures
H_2L_1	362 nm (27624 cm^{-1})	2901	$\pi \longrightarrow \pi^*$	—
	465 nm (21505 cm^{-1})	740	$n \longrightarrow \pi^*$	
CuL_1	332 nm (30120 cm^{-1})	1610	H_2L_1 chromophore ($\pi \longrightarrow \pi^*$)	Square planar
	436 nm (22935 cm^{-1})	1113	Charge transfer (L $\longrightarrow$ M)	
	586 nm (17064 cm^{-1})	40	$^2B_{1g} \longrightarrow {}^2A_{1g}$	
CoL_1	339 nm (29498 cm^{-1})	1137	H_2L_1 chromophore ($\pi \longrightarrow \pi^*$)	Tetrahedral
	476 nm (21598 cm^{-1})	578	Charge transfer (L $\longrightarrow$ M)	
	640 nm (15625 cm^{-1})	176	$^4A_2 \longrightarrow {}^4T_1$ (P)	
NiL_1	329 nm (30395 cm^{-1})	626	H_2L_1 chromophore ($\pi \longrightarrow \pi^*$)	Tetrahedral
	453 nm (22075 cm^{-1})	772	Charge transfer (L $\longrightarrow$ M)	
	564 nm (17730 cm^{-1})	46	$^3T_1(F) \longrightarrow {}^3T_2$ (F)	

$$[Ni^{3+}(C_{17}H_{13}NOS)] + e^- \rightleftharpoons [Ni^{2+}(C_{17}H_{13}NOS)]$$

Scheme 5: Electron transfer process in Ni(II) complex.

indicates the irreversibility of the system. We can only note that the plot of the cathodic potential peak versus the logarithm of scan rate showed a nonlinear relationship (Figure 13) but the cathodic potential depends on the scan rate This indicates that the processes at the surface of the electrodes are slow [42–46]. The cyclic voltammograms of the ligand and its complexes were scanned 20 times at a scan rate of 10 $mV \cdot s^{-1}$ and superposed. Since all the peaks were observed in the same position in all the cycles, it can be concluded that there is no adsorption of the compound on the glassy carbon electrode surface [46].

5. Biological Study

5.1. Antimicrobial Activity of the Ligand and Its Metal Complexes. The Schiff base and its metal complexes were tested against five bacterial strains (*Escherichia coli, Staphylococcus aureus, Pseudomonas aeruginosa, Enterococcus faecalis,* and *Proteus mirabilis)* and five fungi *(Candida albicans*, *Candida glabrata, Candida tropicalis, Candida krusei*, and *Candida parapsilosis*) while Ciprofloxacin and Ketoconazole were used as the standard for bacterial and fungal studies, respectively.

5.1.1. Determination of the Diameters of Zone of the Inhibition (DZI). The diameters of the zone of inhibition of the ligand and its complexes were determined using the agar well diffusion method (Figure 14) [29]. The diameters of zone of inhibition of the bacteria are summarized in Table 6 while Figure 15 is a histogram of the diameter of zone of inhibition.

The results revealed that the synthesized compounds exhibited various levels of inhibition. It was found that the Schiff base H_2L_1 did not show any antibacterial activity against the tested bacterial and fungal strains except *Candida parapsilosis* on which activity is moderate while its metal(II) complexes showed moderate antibacterial activity compared to the ligand but very low compared to the standards used on *Escherichia coli, Staphylococcus aureus, Pseudomonas aeruginosa,* and *Proteus mirabilis* tested. This enhancement in the activity of the metal complexes can be explained on the basis of the chelation theory [47–50]. On chelation, the polarity of the metal ion will be reduced to a greater extent due to the overlap of the ligand orbital and partial sharing of the positive charge of the metal ion with donor groups. Furthermore, the mode of action of the compound may involve the formation of a hydrogen bond through the azomethine group with the active center of cell constituents, resulting in interference with the normal cell process [50].

5.1.2. Minimum Inhibitory Concentration (MIC). The minimal inhibitory concentrations of the compounds were determined using the microdilution in a liquid environment in 96-well microtiter plates [31, 32, 51]. The microbial culture was placed in the presence of the compounds in decreasing order of concentration, in the wells of the microplates. After incubation, the lowest concentration of the antimicrobials in which there was no visible growth of the microorganism represents their minimum inhibitory concentration.

5.1.3. Minimum Bactericidal Concentration (MBC). The minimum bactericidal concentrations of the compounds were determined by sowing 10 μL of the content of every well presenting no manifested change of color after the revelation at the p-iodonitrotetrazolium chloride (INT). After sowing in the sterile boxes of a Petri dish of 90 mm containing MHA, these boxes were incubated at 37°C for 24 hours. At the end of the incubation, the smallest concentration underneath of which no resumption of the bacterial growth was observed is the minimum bactericidal concentration. The minimum inhibitory concentration (MIC) and minimum bactericidal concentration (MBC) results are summarized in Table 7.

5.1.4. Minimum Fungicidal Concentration (MFC). The minimum fungicidal concentrations were obtained by planting out on liquid environment (every well of the 96-well microtiter plate containing 150 μL of culture medium) 50 μL of the content of the wells that did not present any growth.

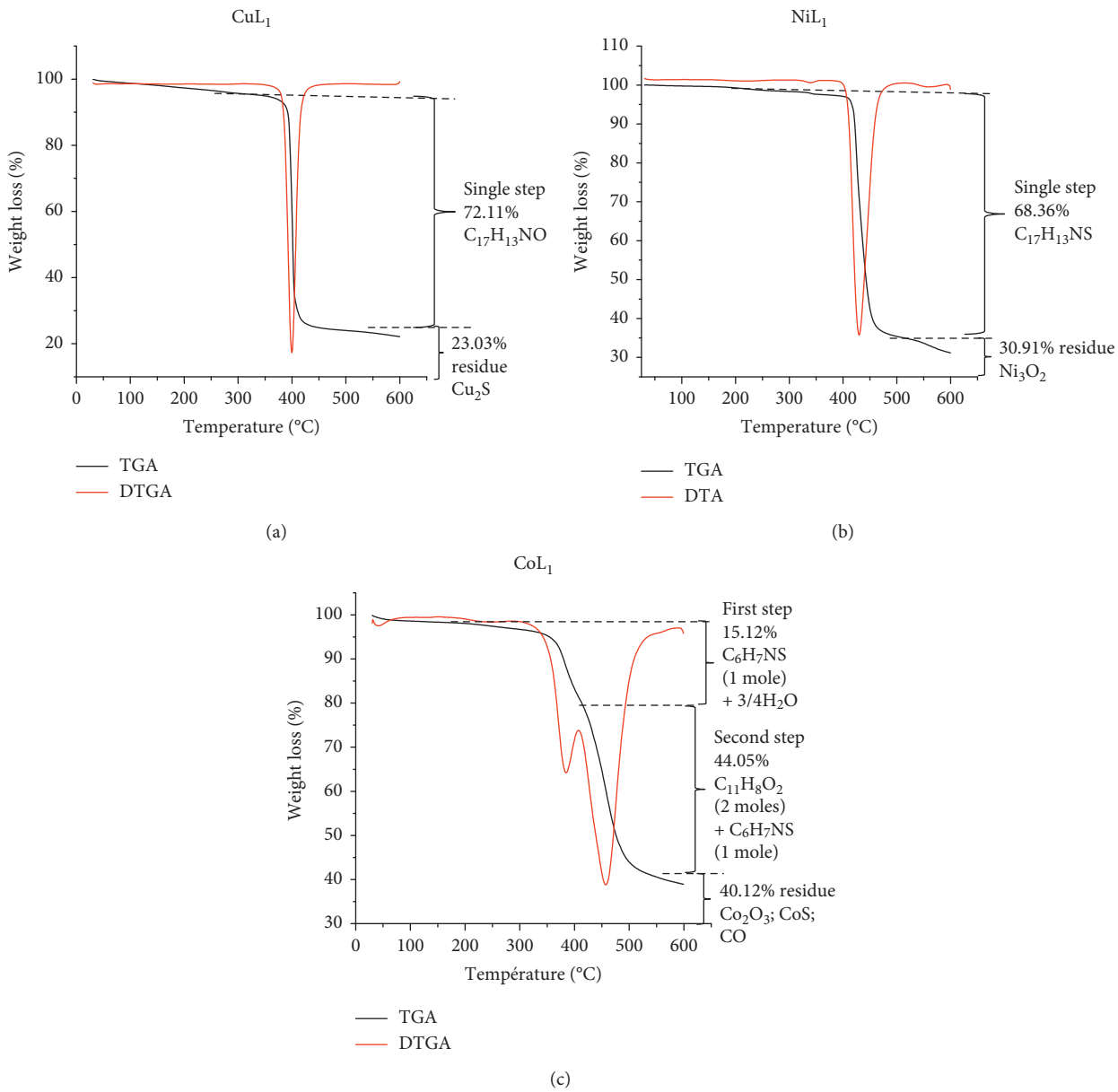

Figure 5: TGA and DTA of CuL_1, NiL_1, and CoL_1 complexes.

Table 5: Thermoanalytical results for CuL_1, CoL_1, and NiL_1 complexes.

Compounds	Step	TGA temperature (°C)	DTA temperature (°C)	Weight loss (%) Found	Weight loss (%) Calc	Process	Fragment lost
CuL_1	Single Residue	385 >600	400 (endothermic)	72.11 23.03	72.56 23.34	Decomposition	$C_{17}H_{13}NO$ (2 moles) Cu_2S
CoL_1	1	220	384 (endothermic)	15.12	15.11	Decomposition	C_6H_7NS (1 mole) + $3/4H_2O$
	2	400–556	457 (endothermic)	44.05	44.10	Decomposition	$C_{11}H_8O_2$ (2 moles) +C_6H_7NS (1 mole)
	Residue	>600	—	40,12	41.52		Co_2O_3; CoS; CO
NiL_1	Single Residue	428 >600	430 (endothermic)	68.36 30.91	68.55 30.96	Decomposition	$C_{17}H_{13}NS$ (2 moles) Ni_3O_2

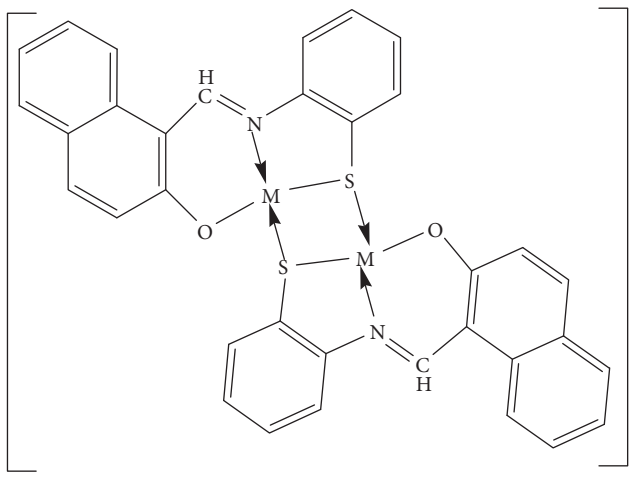

M = Cu^{2+}; Co^{2+}; Ni^{2+}

Figure 6: Proposed structure of the M(II) complexes.

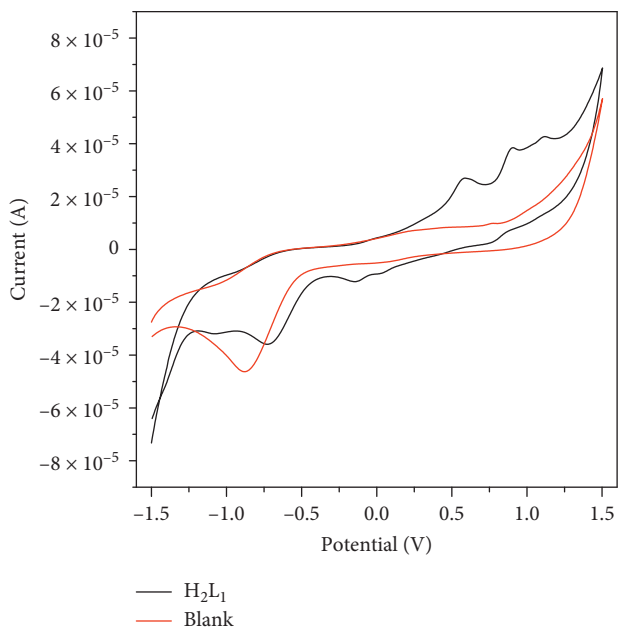

Figure 7: Cyclic voltammogram of blank and ligand H_2L_1.

The smallest concentrations that induced an absence of turbidity at the bottom of the wells after incubation were noted as the minimum fungicidal concentrations. The minimum inhibitory concentration (MIC) and minimum fungicidal concentration (MBC) results are summarized in Table 8.

In Table 8, 256 μg/mL is the minimal value of the concentrations of antifungal and antibacterial in which there is no visible growth of the microorganism.

The activities of compounds are considered significant when MIC and MFC or MBC < 10 μg/mL, moderate when 10 ≤ MIC and MFC or MBC ≤ 256 μg/mL, and weak when MIC and MFC or MBC > 256 μg/mL [50, 51].

It is observed from the biological data that the Schiff base presents weak antifungal activity, except against *C. parapsilosis* where it shows moderate activity with MIC = 64 μg/mL, while the majority of complexes present weak antifungal activities with MIC > 256 μg/mL. The copper complex is weakly active against *Staphylococcus aureus* and *Proteus mirabilis* while the nickel complex is weakly active against *Pseudomonas aeruginosa* and *Proteus mirabilis* The cobalt complex shows weak activity against *Escherichia coli and Staphylococcus aureus*. However, these complexes are significantly more active than the ligand.

5.2. Antioxidant Activity of the Schiff Base and Its Metal Complexes. The synthesized compounds were screened for their free radical scavenging activities by the DPPH method using Trolox as a standard. Antioxidant activities of these

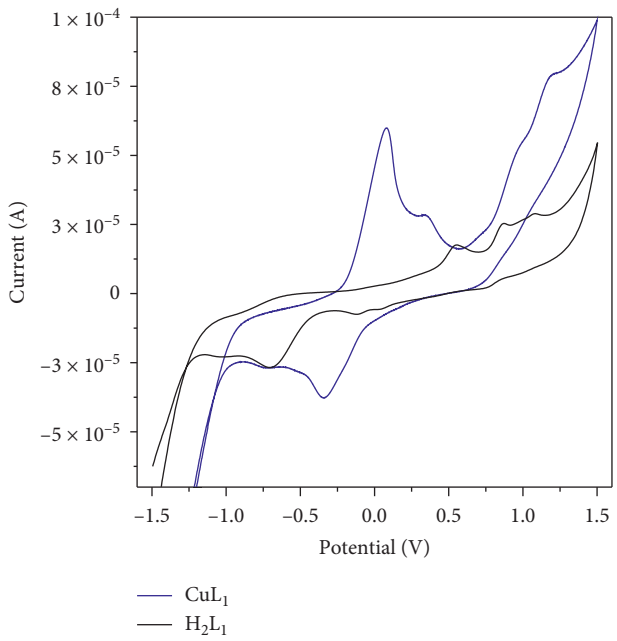

Figure 8: Cyclic voltammograms of Schiff base H_2L_1 and Cu(II) complex.

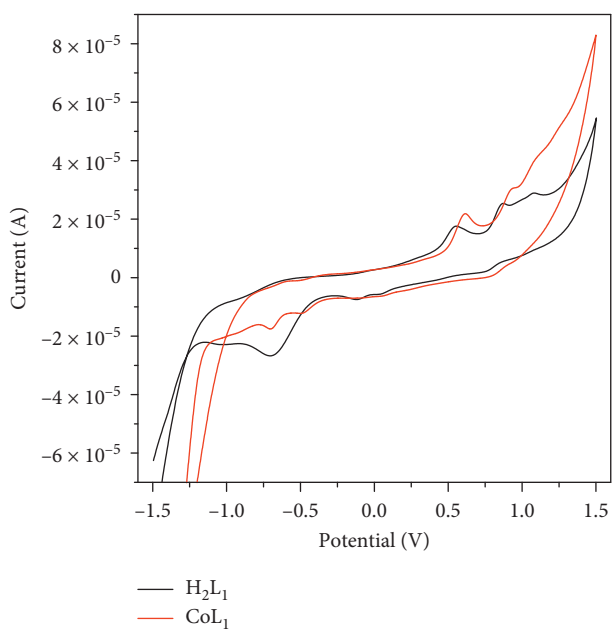

Figure 9: Cyclic voltammograms of Schiff base H_2L_1 and Co(II) complex.

compounds were investigated by measuring the radical scavenging effect on DPPH radicals. The results of the free radical scavenging activity of the compounds at different concentrations are shown in Figure 16. It is evident from these results that the free radical scavenging activities of the compounds are concentration-dependent [49, 52].

The ligand exhibited good scavenging activity. All complexes showed moderate scavenging activity compared to the ligand. This observation could be due to free electron mobility in the complexes [51, 52] and deprotonation of ligand during chelation. The Cu(II) complex exhibited moderate scavenging activity compared to Co(II) and Ni(II) complexes.

EC50 values for scavenging free radicals (Figure 17) confirm the above affirmation that the ligand and its Cu(II) complex are more potent than the Ni(II) and Co(II) complexes.

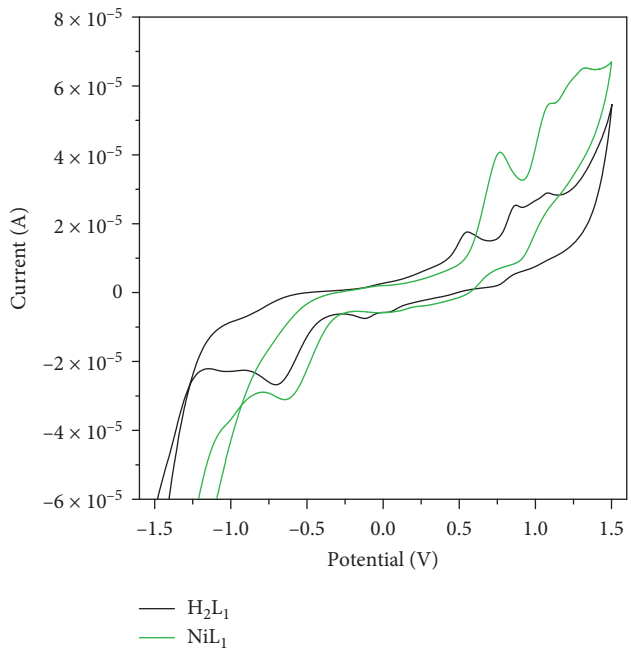

Figure 10: Cyclic voltammograms of Schiff base H_2L_1 and Ni(II) complex.

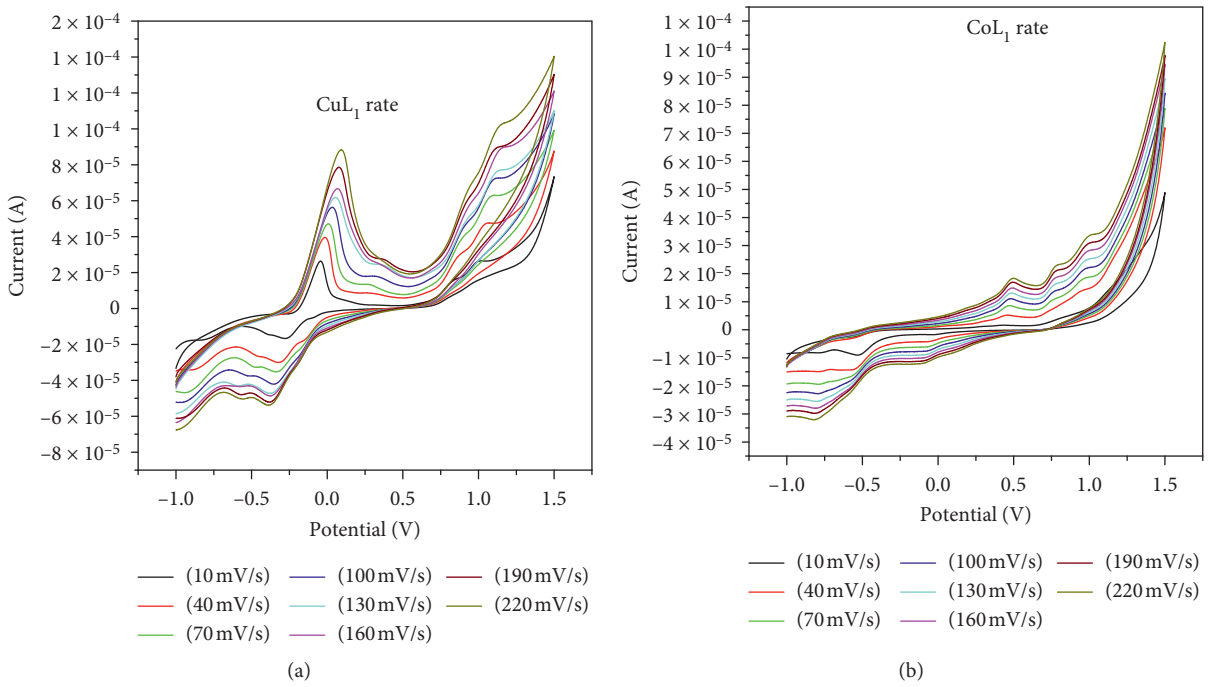

Figure 11: Continued.

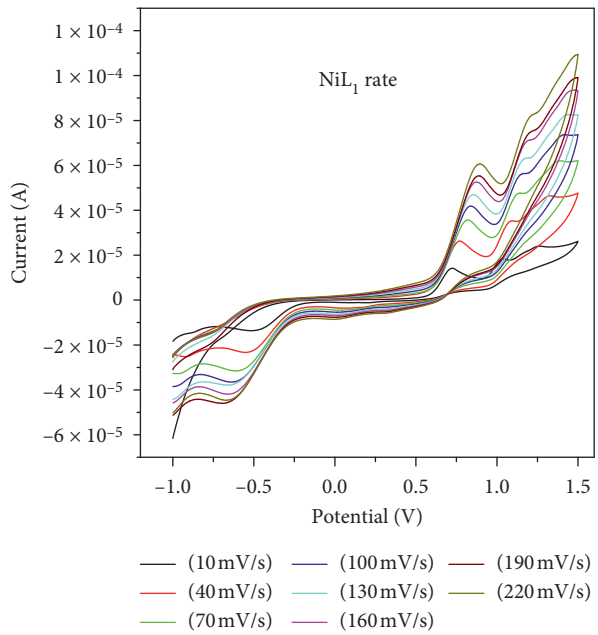

(c)

Figure 11: Scan rates of Cu(II) complex, Co(II) complex, and Ni(II) complex.

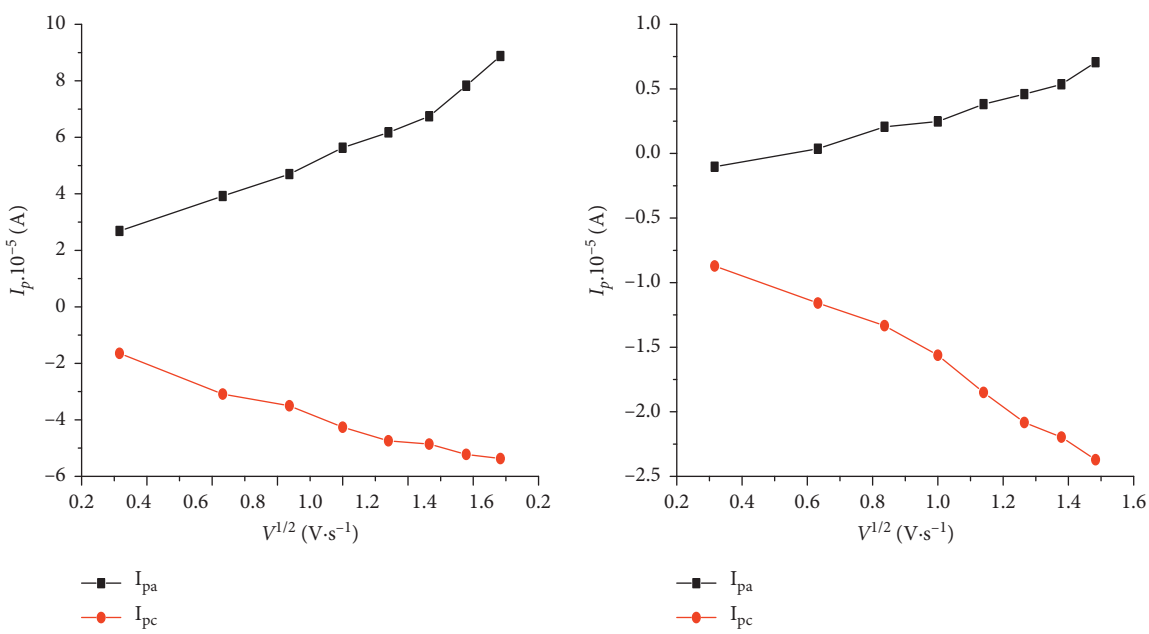

(a) (b)

Figure 12: Continued.

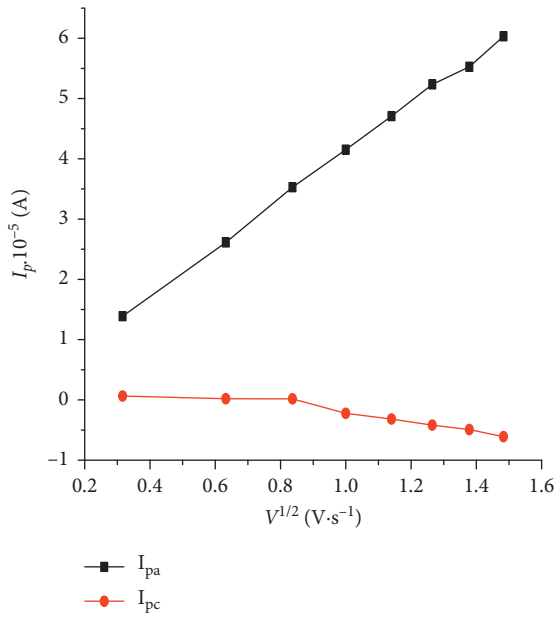

(c)

Figure 12: Plot of I_p versus $v_{1/2}$ for the (a) Cu(II)complex, (b) Co(II)complex, and (c) Ni(II)complex.

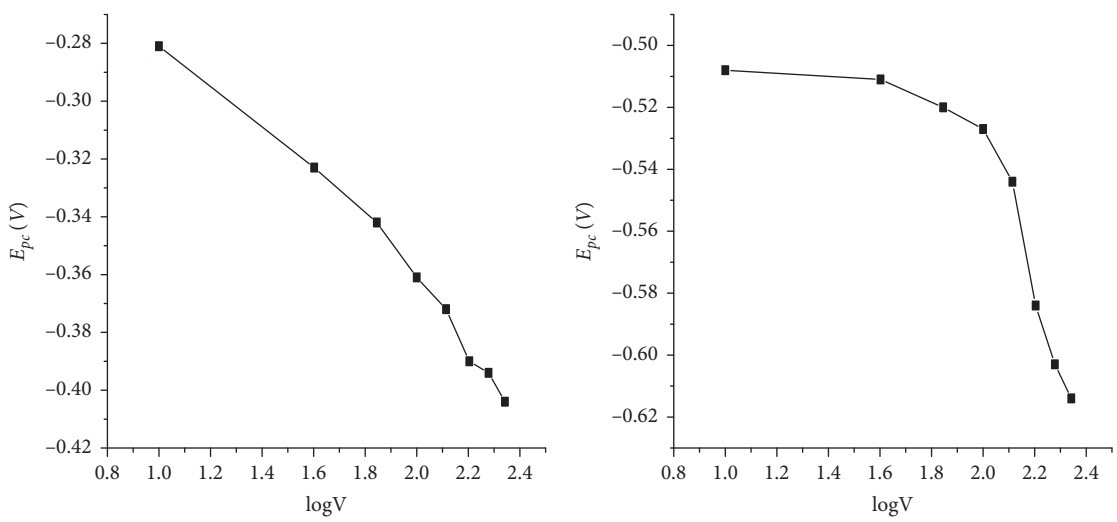

(a) (b)

Figure 13: Continued.

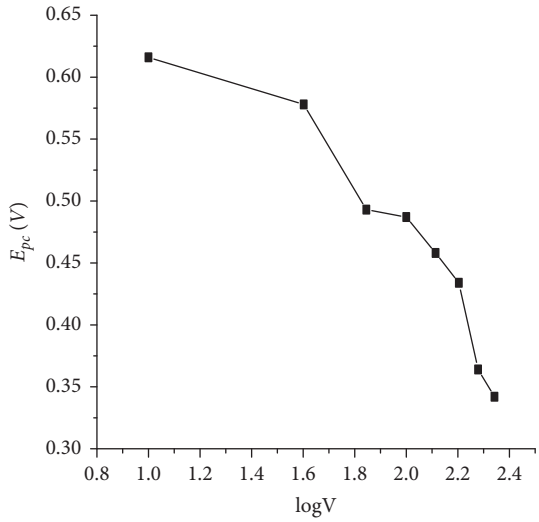

(c)

Figure 13: Plot of E_{pc} versus Log$V$ for the (a) Cu(II)complex, (b) Co(II)complex, and (c) Ni(II)complex.

Figure 14: Antibacterial activity of Schiff base ligand(1) and Cu(II)complex(2), Co(II)complex(3), and Ni(II)complex(4) on *Staphylococcus aureus*.

Table 6: Diameter of the zone of inhibition (DZI) of bacteria.

Bacteria	Diameter of zone of inhibition (DZI)				
	Compounds				Standard
	H_2L_1	CuL_1	CoL_1	NiL_1	Ciprofloxacin
E. coli	—	—	12	—	29
S. aureus	—	13	12	—	39
P. aeruginosa	—	—	—	9	26
E. faecalis	—	—	—	—	29
P. mirabilis	—	10	—	11	30

Compounds are considered active when their diameters of the zone of inhibition are greater than 6 mm (DZI > 6 mm) and (—) no activities are observed.

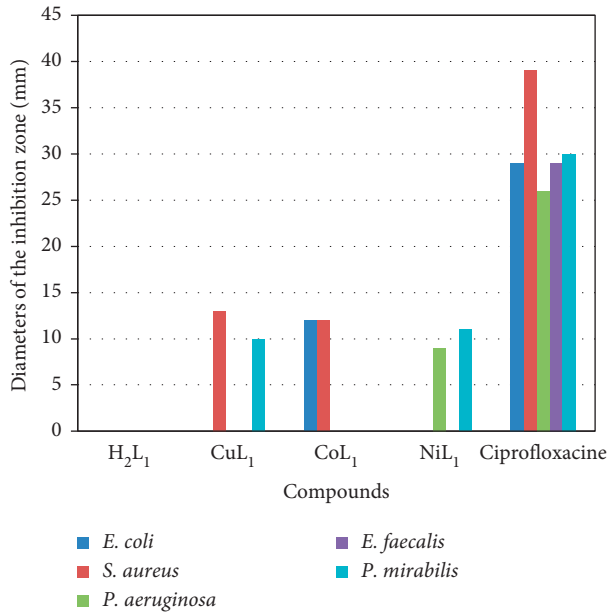

Figure 15: Histogram representing the diameter of zone of inhibition (DZI) in mm of compounds.

Table 7: Minimum inhibition concentration (MIC) and minimum bactericidal concentration (MBC) (μg/mL).

bacteria	Compounds								Standard	
	H_2L_1		CuL_1		CoL_1		NiL_1		Ciprofloxacin	
	MIC	MBC	MIC	MBC	MIC	MBC	MIC	MBC	MIC	MBC
E. coli	>256	>256	32	256	128	>256	128	>256	2	12
S. aureus	>256	>256	32	128	64	256	64	256	1	12
P. aeruginosa	256	>256	64	256	128	>256	64	256	2	8
E. faecalis	256	>256	128	>256	>256	>256	64	256	4	4
P. mirabilis	256	>256	64	256	>256	>256	32	128	2	8

Table 8: Minimum inhibition concentration (MIC) and minimum fungicidal concentration (MFC) (μg/mL).

Fungi	Compounds								Standard	
	H_2L_1		CuL_1		CoL_1		NiL_1		Ketoconazole	
	MIC	MBC	MIC	MBC	MIC	MBC	MIC	MBC	MIC	MBC
C. albicans	256	>256	256	>256	256	>256	256	>256	0.50	64.00
C. glabrata	256	>256	>256	>256	>256	>256	>256	>256	0.25	8.00
C. krusei	256	>256	256	>256	256	>256	>256	>256	0.125	0.50
C. tropicalis	256	>256	256	>256	>256	>256	>256	>256	8.00	8.00
C. parapsilosis	64	256	256	>256	>256	>256	>256	>256	2.00	16.00

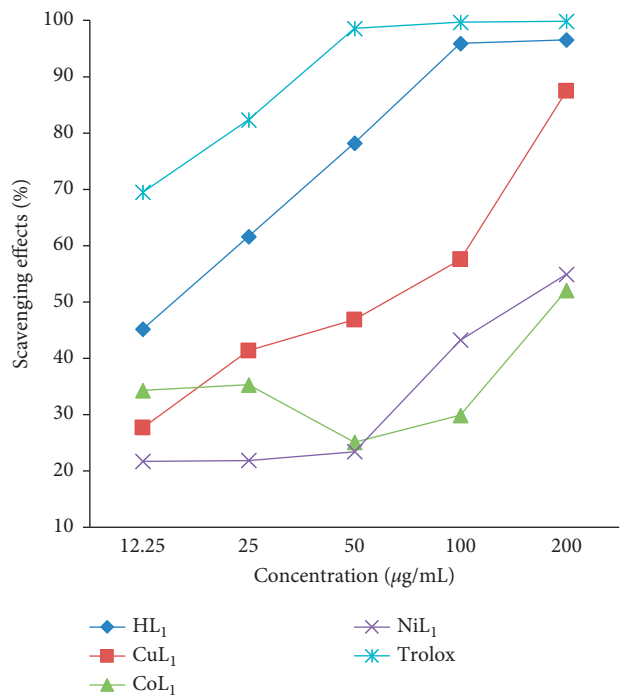

Figure 16: DPPH radical scavenging activity of the ligand and its metal complexes.

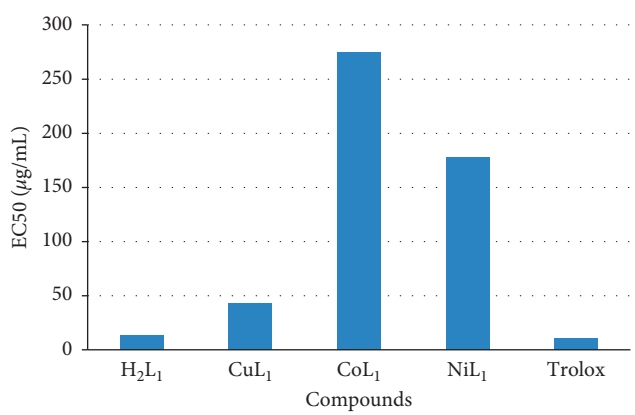

Figure 17: EC50 inhibitory concentration of the H_2L_1 ligand and its metal complexes for 50% of DPPH radical comparison was made against Trolox.

6. Conclusion

We have prepared and characterized a novel tridentate Schiff base ligand (H_2L_1) which coordinates easily to Co(II), Cu(II), and Ni(II) ions to form tetrahedral CoL_1, NiL_1, and square planar CuL_1 complexes. Cyclic voltammetry studies on the ligand and its metal complexes reveal that the redox systems Co(III)/Co(II) and Cu(II)/Cu(I) displayed quasi-reversible processes while Ni(III)/Ni(II) displayed an irreversible process. Antibacterial studies show that the complexes were more active than the free ligand on some bacterial strains while antifungal studies reveal that these compounds showed no antifungal activity. Results of the antioxidant study showed that the ligand and its Cu(II) complex are more efficient to prevent the formation of the DPPH radical than Co(II) and Ni(II) complexes.

Data Availability

All the data used to support the findings of this study are included within the article. Any other data are available from the corresponding author upon request.

Conflicts of Interest

The authors declare that they have no conflicts of interest.

Acknowledgments

The authors acknowledge the Chemistry Department of the University of Zululand for TGA, DTA, and elemental analysis. This work was partly funded under the "Fond de Modernisation et d'Appui a la Recherche" state subsidy to Higher Education University Teachers of Cameroon.

Supplementary Materials

Supplementary Figure 1: IR spectra (4000–400 cm^{-1}) of the ligand, H_2L_1, and its metal complexes. (*Supplementary Materials*)

References

[1] S. Nica, M. Rudolph, I. Lippold, A. Buchholz, H. Görls, and W. Plass, "Vanadium(V) complex with Schiff-base ligand containing a flexible amino side chain: synthesis, structure and reactivity," *Journal of Inorganic Biochemistry*, vol. 147, pp. 193–203, 2015.

[2] L. Xiang and H. Jean-René, "Recent developments in penta-, hexa- and heptadentate Schiff base ligands and their metal complexes," *Coordination Chemistry Reviews*, vol. 389, pp. 94–118, 2019.

[3] J. Rangaswamy, H. Vijay Kumar, S. T. Harini, and N. Naik, "Synthesis of benzofuran based 1,3,5-substituted pyrazole derivatives: as a new class of potent antioxidants and antimicrobials—a novel accost to amend biocompatibility," *Bioorganic & Medicinal Chemistry Letters*, vol. 22, no. 14, pp. 4773–4777, 2012.

[4] E. M. McGarrigle and D. G. Gilheany, "Chromium- and Manganese-salen promoted epoxidation of alkenes," *Chemical Reviews*, vol. 105, no. 5, pp. 1563–1602, 2005.

[5] Z. Guo, R. Xing, S. Liu et al., "Antifungal properties of Schiff bases of chitosan, N-substituted chitosan and quaternized chitosan," *Carbohydrate Research*, vol. 342, no. 10, pp. 1329–1332, 2007.

[6] M. Amjad, S. H. Sumrra, M. S. Akram, and Z. H. Chohan, "Metal-based ethanolamine-derived compounds: a note on their synthesis, characterization and bioactivity," *Journal of Enzyme Inhibition and Medicinal Chemistry*, vol. 31, no. 4, pp. 88–97, 2016.

[7] L. Jian, L. Tingting, C. Sulan, W. Xin, L. Lei, and W. Yongmei, "Synthesis, structure and biological activity of cobalt (II) and copper (II) complexes of valine-derived Schiff bases," *Journal Inorganic Biochemistry*, vol. 100, pp. 1888–1896, 2006.

[8] H. Zahid, M. Arif, A. Muhammad, and T. Supuran, "Metal-based antibacterial and antifungal agents: synthesis, characterization, and in vitro biological evaluation of Co(II), Cu(II), Ni(II), and Zn(II) complexes with amino acid-derived compounds," *Bioinorganic Chemistry and Applications*, vol. 2016, Article ID 083131, 13 pages, 2006.

[9] G. Elif, C. Selma, A. Dilek, and K. Hulya, "Two tridentate Schiff base ligands and their mononuclear cobalt (III) complexes: synthesis, characterization, antibacterial and antifungal activities," *Spectrochimica Acta Part A: Molecular and Biomolecular Spectroscopy*, vol. 94, pp. 216–222, 2012.

[10] P. Ikechukwu and M. Fanyana, "Cu(II) complexes of tridentate Schiff base ligand: synthesis, characterization and biological evaluations," *Medicinal Chemistry*, vol. 7, no. 11, pp. 1–32, 2017.

[11] M. Ashraf, K. Mahmood, and A. Wajid, "Synthesis, characterization and biological activity of Schiff bases," in *Proceedings of the 2011 International Conference on Chemistry and Chemical Process*, Bangkok, Thailand, 2011.

[12] Z. H. Chohan, S. H. Sumrra, M. H. Youssoufi, and T. B. Hadda, "Metal based biologically active compounds: design, synthesis, and antibacterial/antifungal/cytotoxic properties of triazole-derived Schiff bases and their oxovanadium(IV) complexes," *European Journal of Medicinal Chemistry*, vol. 45, no. 7, pp. 2739–2747, 2010.

[13] A. Ekamparam, U. Markandan, and R. Rangappan, "Metal (II) complexes of bioinorganic and medicinal relevance: antibacterial, antioxidant and DNA cleavage studies of tetradentate complexes involving o, n-donor environment of 3, 3′-dihydroxybenzidine-based schiff bases," *International Journal of Pharmacy and Pharmaceutical Sciences*, vol. 5, no. 2, pp. 573–581, 2013.

[14] G. Pandhare, V. Shindea, and Y. Deshpandeb, "Synthesis, characterization and biological studies of cobalt complexes with bidentate Schiff bases," *Rasayan Journal of Chemistry*, vol. 1, no. 2, pp. 337–341, 2008.

[15] M. Kuate, M. A. Conde, K. N. Nchimi, A. G. Paboudam, S.-J. E. Ntum, and P. T. Ndifon, "Synthesis, characterization and antimicrobial studies of Co(II), Ni(II), Cu(II) and Zn(II) complexes of (E)-2-(4-dimethylbenzydimino)-glycylglycine, (glygly-DAB) a schiff base derived from 4-dimethylaminobenzaldehyde and glycylglycine," *International Journal of Organic Chemistry*, vol. 8, no. 3, pp. 298–308, 2018.

[16] A. Wail, "Biological activities of Schiff bases and their complexes: a review of recent works," *International Journal of Organic Chemistry*, vol. 3, pp. 73–95, 2013.

[17] A. Prakash and D. Adhikari, "Application of Schiff bases and their metal complexes—a review," *International Journal ChemTech Research*, vol. 3, no. 4, pp. 1891–1896, 2011.

[18] N. Chaudhary, "In vitro antibacterial studies of some transition metal complexes of Schiff base derived from 2-aminophenol and furan-2-carbaldehyde," *Archives of Applied Sciences and Research*, vol. 5, no. 6, pp. 227–231, 2013.

[19] M. Suman and N. Bharti, "Antimicrobial activities of Schiff bases: a review," *International Journal Theoretical & Applied Sciences*, vol. 8, no. 1, pp. 28–30, 2016.

[20] G. Nizami and R. Sayyed, "Antimicrobial, electrochemical and thermodynamic studies of Schiff base complexes and their potential as anticarcinogenic and antitumor agents: a review," *Journal of Applied Chemistry*, vol. 10, no. 10, pp. 40–51, 2017.

[21] D. Jeyaraj, S. Gurusamy, V. Chinnapiyan, and V. Manokaran, "Synthesis, structural characterization, electrochemical, biological, antioxidant and nuclease activities of 3-morpholinopropyl amine mixed ligand complexes," *Journal of Chemical and Pharmaceutical Research*, vol. 7, pp. 1–14, 2015.

[22] S.-J. E. Ntum, A. G. Paboudam, A. M. Conde et al., "Synthesis and crystal structure of N-(2-pyridylmethyl)-l-alanine) isothiocyanate cobalt(III)," *Crystal Structure Theory and Applications*, vol. 6, no. 3, pp. 39–56, 2017.

[23] S.-J. E. Ntum, B. N. Ndosiri, A. Mohamadou et al., "Synthesis, characterization and X-ray crystal structures of two nonmolecular coordination polymers of manganese(II) and copper(II) with N-(2-pyridylmethyl)-l-alanine and isothiocyanato ligands," *Transition Metal Chemistry*, vol. 41, no. 8, pp. 889–896, 2016.

[24] E. N. Mainsah, S.-J. E. Ntum, M. Samje, F. Cho-Ngwa, P. T. Ndifon, and J. N. Yong, "Synthesis and anti-onchocercal activity of isonicotinoylhydrazones and their copper(II) and

Zinc(II) complexes," *Anti-Infective Agent*, vol. 14, no. 1, pp. 39–56, 2016.

[25] C. Prakasha, M. Raghavendra, R. Harisha, and C. Gowda, "Design, synthesis and antimicrobial screening of amino acids conjugated 2-amino-4-arylthiazole derivatives," *International Journal of Pharmacy and Pharmaceutical Sciences*, vol. 3, pp. 120–122, 2011.

[26] K. Gajendra, K. Dharmendra, D. Shoma, K. Amit, and J. Rajeev, "Synthesis, physical characterization and biological evaluation of schiff base Cr(III), Mn(III) and Fe(III) complexes," *E-Journal of Chemistry*, vol. 7, pp. 813–820, 2010.

[27] L. L. Mensor, F. S. Menezes, G. G. Leitão et al., "Screening of Brazilian plant extracts for antioxidant activity by the use of DPPH free radical method," *Phytotherapy Research*, vol. 15, no. 2, pp. 127–130, 2001.

[28] E. Jaslin and V. Padmaja, "Antioxidant properties and total phenolic content of ethanolic extract of aerial parts of Coleus spicatus Benth," *Journal of Pharmacy Research*, vol. 4, no. 5, pp. 1363-1364, 2011.

[29] V. Berghe and A. Wietinck, "Screening methods for antibacterial and antiviral agents from higher plants," *Methods in Plant Biochemistry*, vol. 6, pp. 47–68, 1991.

[30] S. H. Sumrra and Z. H. Chohan, "Metal based new triazoles: their synthesis, characterization and antibacterial/antifungal activities," *Spectrochimica Acta Part A: Molecular and Biomolecular Spectroscopy*, vol. 98, pp. 53–61, 2012.

[31] S. M. Newton, C. Lau, S. S. Gurcha, G. S. Besra, and C. W. Wright, "The evaluation of forty-three plant species for in vitro antimycobacterial activities; isolation of active constituents from Psoralea corylifolia and Sanguinaria canadensis," *Journal of Ethnopharmacology*, vol. 79, no. 1, pp. 57–67, 2002.

[32] J. A. Kiehlbauch, G. E. Hannett, M. Salfinger, W. Archinal, C. Monserrat, and C. Carlyn, "Use of the national committee for clinical laboratory standards guidelines for disk diffusion susceptibility testing in New York state laboratories," *Journal of Clinical Microbiology*, vol. 38, no. 9, pp. 3341–3348, 2000.

[33] N. U. Mohammad, M. A. Salam, D. A. Chowdhury, and M. B. Siddique, "Binuclear tetrahedral dimeric Mg(II) complexes of dibasictridentate Schiff base ligands and their microbial studies," *CMU Journal of Natural Sciences*, vol. 13, no. 1, pp. 23–35, 2014.

[34] S. Chahmana, S. Keraghel, F. Benghane et al., "Synthesis, spectroscopic characterization, electrochemical properties and biological activity of 1-[(4hydroxyanilino)- methylidene] naphthalen-2(1H)-one and its Mn (III) complex," *International Journal of Electrochemical Science*, vol. 13, pp. 175–195, 2017.

[35] M. Usharani, E. Akila, and R. Rajavel, "Mixed ligand Schiff base complexes: synthesis, spectral characterization and antimicrobial activity," *Journal of Chemical and Pharmaceutical Research*, vol. 4, no. 1, pp. 726–731, 2012.

[36] P. Kanmani, S. Rajalakshmi, and M. Tamilselvi, "Synthesis and spectral analysis of Mn(II), Co(II), Zn(II) and Cd(II) complexes of a new Schiff base derived from p-vanillin and 4-nitroaniline," *International Journal of Innovative Research in Sciences Engineering and Technology*, vol. 7, no. 8, pp. 2229–5518, 2016.

[37] P. R. Chetana, B. S. Srinatha, M. N. Somashekar, and R. S. Policegoudra, "Synthesis, spectroscopic characterisation, thermal analysis, DNA interaction and antibacterial activity of copper(I) complexes with N, N′- disubstituted thiourea," *Journal of Molecular Structure*, vol. 1106, pp. 352–365, 2016.

[38] A. NooriKhaleel and M. Jaafar, "Preparation, characterization and biological study of new boron compound and Schiff base derived from 2-aminophenol with their Cu (II) and Pt (IV) complexes," *IOSR Journal of Applied Chemistry*, vol. 9, no. 8, pp. 4–11, 2016.

[39] A. Kabeer and S. Khaled, "Syntheses, spectral characterization, thermal properties and DNA cleavage studies of a series of Co(II), Ni(II) and Cu(II) polypyridine complexes with some new Schiff-bases derived from 2-chloro ethyl amine," *Canadian Chemical Transaction*, vol. 3, no. 2, pp. 207–224, 2015.

[40] F. Chioma and C. Don-Lawson, "Synthesis, spectral, magnetic and in-vitro biological studies of organic ligands and their corresponding heteroleptic divalent d-metal complexes," *The Pharmaceutical and Chemical Journal*, vol. 5, no. 3, pp. 118–129, 2018.

[41] S. Zolezzi, E. Spodine, and A. Decinti, "Electrochemical studies of copper(II) complexes with Schiff-base ligands," *Polyhedron*, vol. 21, no. 1, pp. 55–59, 2002.

[42] Z. Kadhim, "Synthesis and electrochemical study of Cu(II) complex with neutral [N_2O_2] donor schiff base," *Journal of Materials and Environmental Sciences*, vol. 6, no. 3, pp. 693–698, 2015.

[43] N. Jaishri and B. Rahul, "Synthesis, characterization and electrochemical studies of symmetrical Schiff base complexes of [1-(5 chloro-2-hydroxy-4-methyl- phenyl) ethanone-4-chloro(-3-trifluro methyl) aniline]," *The Pharma Innovation Journal*, vol. 7, no. 1, pp. 149–152, 2018.

[44] A. Salwa, "Synthesis and electrochemical studies of some metal complexes with phosphorus schiff base ligand," *International Journal of Electrochemical Sciences*, vol. 8, pp. 12387–12401, 2013.

[45] A. Kulkarni, S. Patil, and P. Badami, "Electrochemical properties of some transition metal complexes: synthesis, characterization and in-vitro antimicrobial studies of Co(II), Ni(II), Cu(II), Mn(II) and Fe(III) complexes," *International Journal of Electrochemical Sciences*, vol. 4, pp. 717–729, 2009.

[46] K. Shaju, T. Joby, P. Vinod, and N. Kuriakose, "Spectral and cyclic voltammetric studies on Cu(II)-Schiff base complex derived from anthracene-9(10 H)-one," *IOSR Journal of Applied Chemistry*, vol. 7, no. 10, pp. 64–68, 2014.

[47] A. Owolabi and M. Gareth, "Antimicrobial activity and Cu(II) complexes of Schiff bases derived from ortho-aminophenol and salicylaldehyde derivatives," *Journal of Chemistry and Pharmaceutical Research*, vol. 5, no. 10, pp. 147–154, 2013.

[48] R. Mahendra, B. Vivekanand, and B. Mruthyunjayaswamy, "Synthesis, characterization, antimicrobial, DNA cleavage, and antioxidant studies of some metal complexes derived from schiff base containing indole and quinoline moieties," *Bioinorgic Chemistry and Application*, vol. 2013, Article ID 315972, 16 pages, 2013.

[49] S. K. Tadavi, A. A. Yadav, and R. S. Bendre, "Synthesis and characterization of a novel schiff base of 1,2-diaminopropane with substituted salicyaldehyde and its transition metal complexes: single crystal structures and biological activities," *Journal of Molecular Structure*, vol. 1152, pp. 223–231, 2017.

[50] V. Kuete, B. Ngameni, J. G. Tangmouo et al., "Efflux pumps are involved in the defense of Gram-negative bacteria against the natural products isobavachalcone and diospyrone," *Antimicrobial Agents and Chemotherapy*, vol. 54, no. 5, pp. 1749–1752, 2010.

[51] G. Priyadarshini, R. Namitha, D. Mageswari, and G. Selvi, "Synthesis characterization and antioxidant activity of Ni (II) and Co (II) quinoline Schiff base," *International Journal of*

Innovative Research in Sciences Engineering and Technology, vol. 5, no. 1, pp. 101–107, 2016.

[52] P. R. Chetana, M. N. Somashekar, B. S. Srinatha, R. S. Policegoudra, S. M. Aradhya, and R. Rao, "Synthesis, crystal structure, antioxidant, antimicrobial, and mutagenic activities and DNA interaction studies of Ni(II) schiff base 4-methoxy-3-benzyloxybenzaldehyde thiosemicarbazide complexes," *ISRN Inorganic Chemistry*, vol. 2013, Article ID 250791, 11 pages, 2013.